Supplemental Information

Rapid assessment of lipidomics sample purity and quantity using attenuated total reflectance Fourier-transform infrared spectroscopy

Harley Robinson[1], Jeffrey Molendijk[1], Alok K. Shah[1], Tony Rahman[2], Gregory J. Anderson[1], Michelle M. Hill[1,3]

[1] QIMR Berghofer Medical Research Institute, Herston, Brisbane, QLD, Australia 4006

[2] Department of Gastroenterology & Hepatology, The Prince Charles Hospital, Rode Road, Brisbane, QLD 4032

[3] Centre for Clinical Research, Faculty of Medicine, The University of Queensland, Herston, Brisbane, QLD, Australia 4006

Table S1: Distinguishing spectral features in biological molecules. A collection of the most distinctive vibrational frequencies (in wavenumber) detected in tested biological molecules, with biological interpretations and chemical structure descriptions.

Structural and compositional regions	**Wavenumber** (cm^{-1})	**Molecule type**	**Supporting References**
Hydrocarbon **CH3** (stretching) **CH2 (**stretching**)** **CH** (alkane, stretching**)** **CH** (alkene, stretching) **CH** (bending)	 2958 2922 2925 3080 1450	Enriched in lipid, detergent. Contained in most organic molecules. Alkenes increase in unsaturated lipid.	[26]
Carbonyl (C=O) **Carboxyl** (C=OOH) **Ester** (C=OOC**)**	 1710 1740	Fatty acids (carboxyl) Lipids (ester)	[22, 27]
Amide **Amide A** (NH- stretching) **Amide I** (NH-bending) **Amide II (**NH-bending)	 3525 1654 1550	Protein, peptide (amide), nucleic acids (amine)	[21, 28]
Fingerprint region **COH** (hydroxyl, stretching) **CO** (stretching) **PO2-** (stretching, asymmetric) **PO2-** (stretching, symmetric)	 1160 1051, 1160 1245 1080	Saccharide, glycosphingolipids, nucleic acids, phospho-groups.	[28-30]

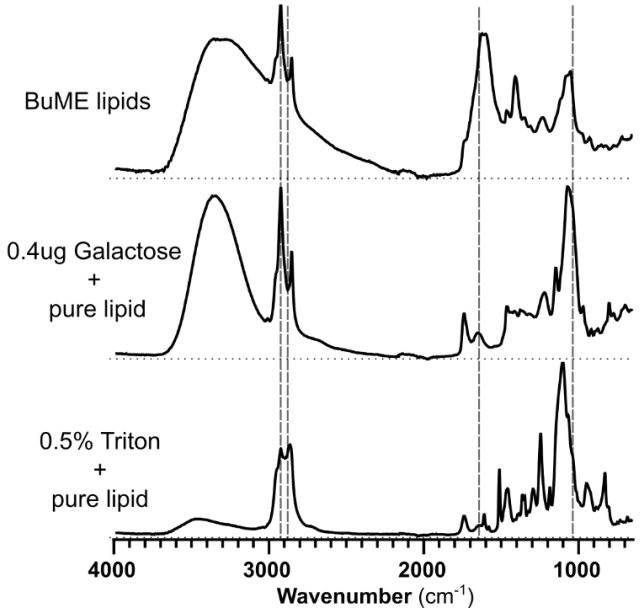

B

LiQ score	Spectral feature ratio		
$\frac{CH_{max}}{(CH_{min} + Amide + "Sugar")}$	$\frac{CH_{max}}{CHmin}$	$\frac{CH_{max}}{Amide}$	$\frac{CH_{max}}{"Sugar"}$
0.58 (+/- 0.02)	1.76 (+/- 0.03)	1.67 (+/- 0.06)	2.40 (+/- 0.10)
0.69 (+/- 0.01)	2.28 (+/- 0.03)	7.50 (+/- 0.61)	1.19 (+/- 0.05)
0.53 (+/- 0.02)	1.09 (+/- 0.09)	10.96 (+/- 0.54)	1.18 (+/- 0.09)

Figure S1: Complementary measurements for LiQ score quality control analysis. A) Stacked spectra of BuMe extracted lipids, and lipid samples contaminated with 0.5% Triton-X100, or 0.4µg galactose per 1µg TBME extracted lipid. Vertical dotted lines highlight the important spectral regions, specifically, CH_{max}, CH_{min}, Amide I, and "Sugar" regions. **B)** Comparison of LiQ scores and spectral feature ratios as metrics of lipid purity. Despite similar LiQ scores across each spectrum, the ratios of spectral features indicate the presence of contaminants, which is not ideal.

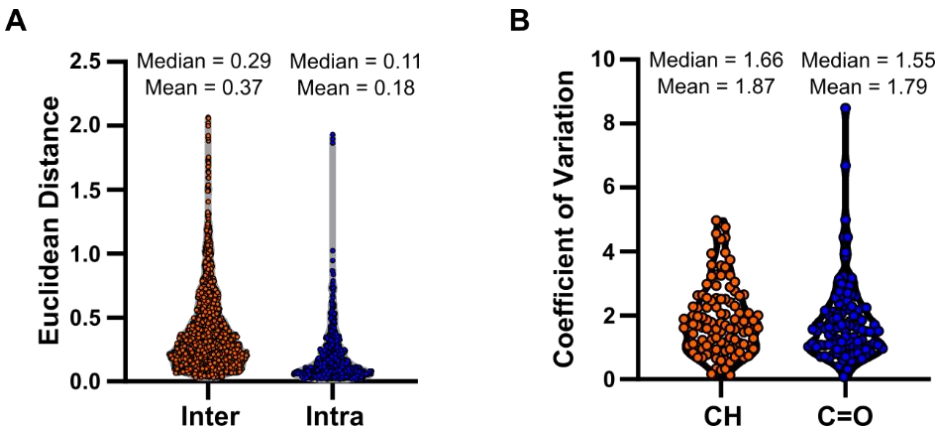

Figure S2: Variation in technical and biological replicates. 3-5 technical replicates were measured for all 107 human plasma samples. **A)** The variation between technical replicates (intra-sample variation) and between biological replicates (inter-sample variation) measured by Euclidean distance. **B)** Coefficient of variation for the measured AUCs for CH and C=O region for each biological replicate.

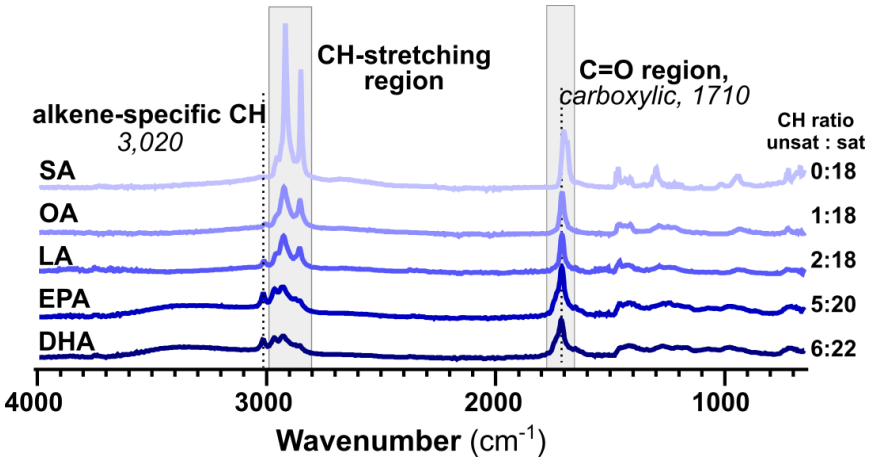

Figure S3: Variations in the CH region by unsaturated fatty acids. FTIR spectra of polyunsaturated fatty acids. Unsaturation to chain ratio shown on the right. Equal amount of lipid was measured for each (625ng). Fatty acids measured are Stearic acid (SA), Oleic acid (OA), Linoleic acid (LA), Eicosapentaenoic acid (EPA), Docosahexaenoic acid (DHA), all purchased from Sigma-Aldrich. Unsaturated lipids gain an alkene specific CH peak while reducing the prevalent peaks in the saturated lipid CH region, while lipid carboxyl regions (C=O) remain uniform.

Supplementary references

21. Fellows, A.P., M.T.L. Casford, and P.B. Davies, *Spectral Analysis and Deconvolution of the Amide I Band of Proteins Presenting with High-Frequency Noise and Baseline Shifts.* Appl Spectrosc, 2020. **74**(5): p. 597-615.
22. Forfang, K., et al., *FTIR Spectroscopy for Evaluation and Monitoring of Lipid Extraction Efficiency for Oleaginous Fungi.* PLOS ONE, 2017. **12**(1): p. e0170611.
26. Versteegh, G., A.J.P. Houben, and K. Zonneveld, *Better molecular preservation of organic matter in an oxic than in a sulfidic depositional environment: evidence from Thalassiphora pelagica (Dinoflagellata, Eocene) cysts.* Biogeosciences, 2020. **17**: p. 3545-3561.
27. Filopoulou, A., S. Vlachou, and S.C. Boyatzis, *Fatty Acids and Their Metal Salts: A Review of Their Infrared Spectra in Light of Their Presence in Cultural Heritage.* Molecules, 2021. **26**(19).
28. Rolim, T., J. Cancino, and V. Zucolotto, *A nanostructured genosensor for the early diagnosis of systemic arterial hypertension.* Biomedical microdevices, 2015. **17**: p. 9911.
29. Ensari, Ö., *Polyethylene Glycol-Sugar Composites as Shape Stabilized Phase Change Materials for Thermal Energy Storage.* Polymer Composites, 2012. **33**: p. 1728-1736.
30. Wang, T., et al., *Detection of endogenous biomolecules in Barrett's esophagus by Fourier transform infrared spectroscopy.* Proceedings of the National Academy of Sciences of the United States of America, 2007. **104**: p. 15864-9.